Combined Convection In a TSNFL Square Cavity Under Various Moving Wall Directions

الحمل المشترك لفجوة مربعة ذات جانبين غير متقابلين ومتحركين في اتجاهات مختلفة لحركة جدران الفجوة

Ahmed Kadhim Hussein

College of Engineering -Mechanical Engineering Department -Babylon University - Babylon City – Hilla – Iraq.

E-mail ahmedkadhim74@ yahoo.com

Abstract:

   Laminar combined convection air flow in a two-sided non-facing lid-driven (TSNFL) square cavity has been investigated numerically using a finite element method. The upper and lower walls are maintained at constant cold and hot temperatures respectively, while the left and right side walls are considered adiabatic. Four groups are considered for the movements of the TSNFL cavity walls and each group contains four different cases. All the non-facing cavity walls are considered to move at a constant lid velocity. Simulation of the cavity flow has been performed at three different Richardson numbers representing the natural convection, combined convection, and forced convection. The effect of the Richardson number and the movements of the TSNFL cavity walls on the heat transfer process are studied. The results are presented graphically in the form of streamlines, isotherms and average Nusselt number. The results indicated that the vortices grow with the direction of the movements of TSNFL cavity walls and the average Nusselt number decreases when the Richardson number increases. The results are compared with another published result and a good agreement are obtained.

Key words**:** Combined convection **,** TSNFL , FEM , Steady flow .

الملخص :

   الحمل المشترك الطباقي لجريان الهواء في فجوة مربعة ذات جانبين غير متقابلين ومتحركين تم نمذجته عدديا باستخدام طريقة العناصر المحددة .يتعرض الجداران العلوي والسفلي لدرجات حرارة باردة وساخنة بالتعاقب بينما الجدران الجانبيان الأيمن والأيسر معزولين حراريا.أربعة مجاميع لحركة جدران الفجوة الغير المتقابلة تم دراستها وكل مجموعة تحتوي أربعة حالات مختلفة .جميع الجدران الغير متقابلة تتحرك بسرعة ثابتة .نمذجة الجريان داخل الفجوة تم دراسته لثلاث قيم لرقم ريكاردسون تمثل الحمل الحر , الحمل المشترك والحمل القسري.تأثير رقم ريكاردسون واتجاهات حركة جدران الفجوة الغير المتقابلة على عملية انتقال الحرارة تم دراستها.النتائج تم استعراضها على شكل مخططات لخطوط الجريان والحرارة ورقم نسلت المتوسط.النتائج بينت أن الدوامات تتشكل مع أتجاهة حركة الجدران الغير المتقابلة وان رقم نسلت المتوسط يتناقص بزيادة رقم ريكاردسون.النتائج تم مقارنتها بنتائج أخرى منشورة ولوحظ وجود تطابق جيد بين الاثنين.

1. Introduction

   Laminar combined convection flow in an enclosure driven by moving boundaries is perhaps one of the most significant problem encountered in the thermal engineering field. This type of flow can be found in various engineering applications such as furnace, drying technologies, solar ponds and thermal hydraulics of nuclear reactors. A classic problem is the case where a flow is induced by the tangential movement of either one or both facing cavity boundaries .One-sided lid-driven flow in a cavity was studied extensively in the literature. Numerous studies have been conducted in the past on combined convection involving different enclosure configurations, various fluids and imposed temperature gradients for example , **Moallemi** and **Jang [1]** , **Alleborn et al. [2]** , **Mahapatra et al. [3]** , **Wahba [4-5]** and **Alinia et al. [6]**. **Mansour** and **Viskanta [7]** investigated combined convection in a narrow vertical cavity, where one vertical wall was cooled and moved upward, such that the shear forces induced by the wall motion oppose the buoyant force. **Oztop** and

Dagtekin [8] investigated numerically two-dimensional mixed convection problem in a vertical lid-driven enclosure. They observed that Richardson number affected the flow and heat transfer in the enclosure. **Mahapatra et al. [9]** investigated numerically opposing mixed convection in a differentially heated partitioned enclosure. It was found that when height of centrally located partition increased , the heat transfer was found to be more than that of natural convection for a partitioned enclosure. **Luo** and **Yang [10]** simulated numerically the fluid flow and heat transfer in a TSNFL cavity with an aspect ratio of 1.96. They concluded that for higher values of Reynolds number, two saddle-node points were identified on the corresponding branches. **Beya** and **Lili [11]** presented a numerical simulations of the three-dimensional fluid flow in a two-sided cubical cavity. The time dependent solution was studied and the critical Reynolds number was localized. **Siegmann-Hegerfeld et al. [12]** investigated experimentally two and three-dimensional flows in rectangular cavities driven by collinear motion of two facing walls. The critical thresholds for the onset of most of the three-dimensional modes had been observed which agreed with corresponding linear-stability calculations. **Basak et al. [13]** used finite element simulations to investigate the influence of linearly heated side wall(s) or cooled right wall on combined convection lid-driven flows in a square cavity. It was observed that multiple circulation cells appeared inside the cavity with the increase of Prandtl number. **Noor et al. [14]** studied the flow in a square cavity with double-sided oscillating lids in anti-phase. They concluded that the heat transfer rates were affected by non-dimensional oscillation angular frequency. **Ouertatani et al. [15]** studied three-dimensional combined convection in double lid-driven cubic cavity heated from the top and cooled from below. It was found that a remarkable heat transfer improvement of up to 76% could be reached for the particular combination of Re = 400 and Ri =1. **Cheng** and **Liu [16]** investigated the effect of temperature gradient orientation in a lid-driven differentially heated square cavity. It was found that the direction of temperature gradient affected the flow in the cavity. **Oueslati et al. [17]** carried a numerical study of the three-dimensional fluid flow in two-sided cavities. A correlation was established and gave the critical Reynolds number value. **Vicente et al. [18]** studied two-dimensional laminar flows in a span wise-periodic double-sided lid-driven cavity with complex cross-sectional profiles. Neutral loops were established for the geometries considered. **Golkarfard et al. [19]** investigated numerically the laminar combined convection flow in a lid-driven cavity with two heated obstacles. They concluded that the size of obstacles had a great effect on particle deposition. **Cheng et al. [20]** investigated numerically the mixed convection in a 2-D cavity .The average Nusselt numbers were reported to illustrate the influence of flow parameter variations on heat transfer process. The present work studied the case of TSNFL cavity in which the flow is driven by the TSNFL cavity walls in all directions.

2. Mathematical Model.

The configuration for the TSNFL square cavity filled with air (Pr = 0.71) is sketched in Fig.1. The cavity left and right sidewalls are considered adiabatic. The upper wall is maintained at constant cold temperature (T_c) while the lower wall is maintained at constant hot temperature (T_h). The flow inside the cavity is driven by the movements of the TSNFL cavity walls, which move with equal velocities in different directions. Four groups are considered for the movements of the TSNFL cavity walls and each group contains four cases which are :-

Group A
Case I :The upper wall moves at a constant velocity (V_c) from right to left , while the right adiabatic sidewall moves downwards at the same velocity.
Case II :The upper wall moves at a constant velocity (V_c) from left to right , while the left adiabatic sidewall moves downwards at the same velocity.
Case III :The lower wall moves at a constant velocity (V_c) from left to right , while the left adiabatic sidewall moves upwards at the same velocity.
Case IV : The lower wall moves at a constant velocity (V_c) from left to right , while the right adiabatic sidewall moves upwards at the same velocity.

Group B

Case I : The upper wall moves at a constant velocity (V_c) from left to right , while the right adiabatic sidewall moves upwards at the same velocity.

Case II :The lower wall moves at a constant velocity (V_c) from left to right , while the right adiabatic sidewall moves downwards at the same velocity.

Case III :The upper wall moves at a constant velocity (V_c) from left to right , while the left adiabatic sidewall moves upwards at the same velocity.

Case IV : The lower wall moves at a constant velocity (V_c) from left to right , while the left adiabatic sidewall moves downwards at the same velocity.

Group C

Case I : The upper wall moves at a constant velocity (V_c) from left to right , while the right adiabatic sidewall moves downwards at the same velocity.

Case II :The upper wall moves at a constant velocity (V_c) from right to left , while the left adiabatic sidewall moves downwards at the same velocity.

Case III :The lower wall moves at a constant velocity (V_c) from right to left , while the right adiabatic sidewall moves upwards at the same velocity.

Case IV : The lower wall moves at a constant velocity (V_c) from right to left, while the left adiabatic sidewall moves upwards at the same velocity.

Group D

Case I : The upper wall moves at a constant velocity (V_c) from right to left , while the right adiabatic sidewall moves upwards at the same velocity.

Case II :The upper wall moves at a constant velocity (V_c) from left to right , while the left adiabatic sidewall moves upwards at the same velocity.

Case III :The lower wall moves at a constant velocity (V_c) from right to left , while the right adiabatic sidewall moves downwards at the same velocity.

Case IV : The lower wall moves at a constant velocity (V_c) from right to left, while the left adiabatic sidewall moves downwards at the same velocity.

The governing parameter is Richardson number which is varied from 0.01 to 100. To vary Richardson number, Grashof number is considered fixed at $Gr = 10^4$ while changing Reynolds number through the lid velocity (V_c) so that the range of Reynolds number is taken as ($10 \leq Re \leq 1000$).

The following assumptions are considered in the present work : -

1.The flow is assumed two-dimensional , Newtonian , laminar and steady.

2.The fluid properties are assumed constant except the density variation.

3.The viscous dissipation effects are considered negligible.

The governing equations are converted into a dimensionless forms by using the following dimensionless variables:

$$\theta = \frac{T - T_c}{\Delta T} \ , \quad U, V = \frac{u, v}{V_c} \ , \quad P = \frac{p}{\rho V_c^2} \ , \quad X, Y = \frac{x, y}{H} \tag{1}$$

Therefore, the dimensionless governing equations of present work are expressed in the following forms:

$$U_x + V_y = 0 \tag{2}$$

$$UU_x + VU_y = -P_x + \left(\frac{Gr}{Ri}\right)^{-0.5}(\nabla^2 U) \tag{3}$$

$$UV_x + VV_y = -P_y + \left(\frac{Gr}{Ri}\right)^{-0.5}(\nabla^2 V) + Ri\theta \tag{4}$$

$$\mathrm{U}\theta_x + \mathrm{V}\theta_y = \frac{1}{\mathrm{Pr}}(\frac{Gr}{Ri})^{-0.5}(\nabla^2\theta) \tag{5}$$

The Richardson number is defined as :-

$$\mathrm{R}i = \frac{g\beta(T_h - T_c)H^3}{\nu^2 \mathrm{Re}^2} \tag{6}$$

The heat transfer rate is expressed in terms of average Nusselt number at the hot lower wall as follows:-

$$\overline{Nu}_h = -\int_0^1 (\frac{\partial\theta}{\partial Y})\mathrm{d}Y \tag{7}$$

Boundary conditions : The dimensionless boundary conditions which are used in the present study can be arranged as follows:-

1.The upper wall is maintained at constant cold temperature (T_c) sliding at a constant velocity (V_c) in the left and right directions so that :-

at Y=1 and $0 < X < 1$, $\theta = 0$, $\Psi = 0$ for stationary wall and $U = \mp 1$ for lid wall

2.The lower wall is maintained at constant hot temperature (T_h) sliding at a constant velocity (V_c) in the left and right directions so that :-

at Y=0 and $0 < X < 1$, $\theta = 1$, $\Psi = 0$ for stationary wall and $U = \mp 1$ for lid wall

3.The left sidewall is considered adiabatic and sliding at a constant velocity (V_c) in the upward and down ward directions so that :-

at X=0 and $0 < Y < 1$, $\frac{\partial\theta}{\partial X} = 0$, $\Psi = 0$ for stationary wall and $V = \mp 1$ for lid wall

4.The right sidewall is considered adiabatic and sliding at a constant velocity (V_c) in the upward and down ward directions so that :-

at X=1 and $0 < Y < 1$, $\frac{\partial\theta}{\partial X} = 0$, $\Psi = 0$ for stationary wall and $V = \mp 1$ for lid wall

3. Numerical method , grid test and validation

The finite element method is used to discretize the non-dimensional Navier-Stokes and energy equations (Eqs.(2-5)). The details of this algorithm and the mesh generation procedure are given by **Liu** and **Quek [21]**. A program code is written in Fortran language to follow this algorithm. An iterative process by the line-by-line method solves each variable obtained from the resulting set of discretized governing equations. The iteration process is repeated until the convergence criterion is satisfied when the values of residual terms in the momentum and energy equations did not exceed 10^{-7}. In order to obtain a grid-independent solution , eight combinations (40 x 40, 50 x 50, 60 x 60, 70 x 70, 80 x 80, 100 x 100, 128 x 128 and 150 x 150) of non-uniform grids are used to check the influence of grid size on the accuracy of the computed results. Fig.2 shows the convergence of the average Nusselt number ($\overline{Nu}_h$) with grid refinement. It is observed that the grid independence occurs with a grid set of (128 x128). The accuracy of present computer code has been verified by considering the combined convection problem in a lid-driven cavity with a stable vertical temperature gradient considered by **Oztop** and **Dagtekin [8]**. It can be seen from **Table 1**, that there is a good agreement for average Nusselt numbers at the top wall obtained by the present computer code when compared with their corresponding values considered by **Oztop** and **Dagtekin [8]** with a maximum difference of about 0.953 %.

4. Results and Discussion.

4.1. The forced convection effect , (i.e., Ri = 0.01)

Figures **3** and **4** show the streamlines and isotherms when the forced convection effect is dominated (i.e., Ri = 0.01) for various TSNFL cavity orientations. In this case, the shear force due

to the movements of the TSNFL cavity walls has a stronger influence compared with buoyancy force. The results are discussed as follows :-

1-It can clearly see that when the upper wall moves to the left and when the right side wall moves downwards , a two large separate major clockwise and anti-clockwise vortices can be generated which occupy the core of the flow and its size increases with the increase of the movements of these TSNFL cavity walls. This is because the convection currents begin from the lower hot wall and move towards the upper cold wall due to buoyancy and shear forces. Also, a small minor re-circulating clockwise and anti-clockwise vortices can be observed at the lower edge of the cavity. The same behavior can be observed when the direction of the movements of the TSNFL cavity walls diverges (for example, when the upper wall moves to the right and the left side wall moves downwards or when the lower wall moves to the right and the left side wall moves upwards , etc.).The only difference is that the large major vortices grow with the direction of the movements of TSNFL cavity walls. The maximum stream function at these cases is about ($\Psi_{Max} = 0.1660$).With respect to isotherms, there is a clear concentrations of them adjacent the upper cold and the lower hot corners of the cavity. This is due to the strong temperature gradient in the vertical direction which gives an indication that the convection heat transfer becomes more significant compared to the conduction heat transfer.

2-When the direction of the movements of the TSNFL cavity walls converges (for example, when the upper wall moves to the right and the right side wall moves upwards or when the upper wall moves to the left and the left side wall moves upwards , etc.) , a two large major clockwise and anti-clockwise vortices can be seen with a perfectly symmetrical patterns about the diagonal of the cavity. In this case , the minor vortices are begin to disappear from the flow field. The maximum stream function at these cases is about ($\Psi_{Max} = 0.2118$). With respect to isotherms, the concentration of them adjacent the cold upper and hot lower walls increases when the direction of the movements of the TSNFL cavity walls converges. In this case, the isotherms begin to shift towards the diagonal of the cavity. This is due to the strong effect of both the shear and buoyancy forces.

3-When the direction of the movements of the TSNFL cavity walls is in the clockwise direction (for example, when the lower wall moves to the left and the right side wall moves downwards or when the upper wall moves to the right and the right side wall moves downwards , etc.) , the flow field structure can be characterized by a large single major vortices at the center of the cavity. Also, a small single minor vortices can be noticed at the cavity corner. The maximum stream function at these cases is about ($\Psi_{Max} = 0.1454$).The same behavior can be seen when the movements of the TSNFL cavity walls is in the anti-clockwise direction (for example, when the lower wall moves to the right and the right side wall moves upwards or when the upper wall moves to the left and the right side wall moves upwards , etc.).The maximum stream function are observed to be ($\Psi_{Max} = 0.1457$). With respect to isotherms, it can be noticed that they are clustered adjacent the cavity corners and a thermal boundary layer can be noticed at these regions. By comparing the results of these various cases , it can be seen that the case where the direction of the movements of the TSNFL cavity walls converges provides a high circulation intensity of the flow field compared with another considered cases. The reason of this behavior, since at this case the shear and buoyancy forces act in the same direction. In general, when the Richardson number is very low (i.e., Reynolds number is high) , the isotherm contours take a confusion shape and a high disturbance can be seen in it where the convection heat transfer is dominant.

4.2. The combined convection effect (i.e., Ri = 1)

Figures **5** and **6** illustrate respectively the streamlines and isotherms when the forced convection effect is approximately equivalent to the natural convection effect (i.e., Ri =1) for various TSNFL cavity orientations. In this case, the shear force has the same influence with the buoyancy force. The results are discussed as follows :-

1-When the direction of the movements of the TSNFL cavity walls diverges (for example, when the upper wall moves to the right and the left side wall moves downwards or when the lower wall moves to the right and the left side wall moves upwards , etc.).One of the major large vortices begins to grow and extends clearly inside the cavity, while the other major large vortices which are observed when the Richardson number is very low begins to decrease in size. From the other hand, the minor vortices which are noticed adjacent the cavity corners begin to decrease also if it compared with the corresponding minor vortices when the Richardson number is very low. Also, the circulation intensity decreases due to decrease the role of the shear force when the Richardson number increases from 0.01 to 1.0.This increasing in the Richardson number reduces the influence of the movements of the TSNFL cavity walls and causes to reduce the circulation intensity. The maximum stream function at these cases is about ($\Psi_{Max} = 0.01836$).

2-When the direction of the movements of the TSNFL cavity walls converges (for example, when the upper wall moves to the right and the right side wall moves upwards or when the upper wall moves to the left and the left side wall moves upwards , etc.) , the flow field can be represented by a two major vortices which are symmetrical in shape but they are different in size. It can also be seen that the maximum stream function increases from ($\Psi_{Max}=0.01836$) when the direction of the movements of the TSNFL cavity walls diverges to ($\Psi_{Max}=0.01945$) when the direction of the movements of the TSNFL cavity walls converges. This is because, the buoyancy and shear forces act in the same direction. From the other side, the minor vortices are completely disappear from the flow field at this case.

3-When the direction of the movements of the TSNFL cavity walls is in the clockwise direction (for example, when the lower wall moves to the left and the right side wall moves downwards or when the upper wall moves to the right and the right side wall moves downwards , etc.) , the flow field structure can be represented by a large single major vortices which occupy the entire cavity zone. In this case , it can be seen that the center of the vortices are shifted either in the upwards direction or in the downwards direction according to the orientation of the movements of the TSNFL cavity walls. From the other side, a very small minor vortices can be found in the upper or lower corners of the cavity. The maximum stream function at these cases is about ($\Psi_{Max} = 0.01927$). The same behavior can be seen when the movements of the TSNFL cavity walls is in the anti-clockwise direction (for example, when the lower wall moves to the right and the right side wall moves upwards or when the upper wall moves to the left and the right side wall moves upwards , etc.).The maximum stream function are observed to be ($\Psi_{Max} = 0.02031$). With respect to isotherms, the disturbance in the isotherm contours begin to decrease gradually when the Richardson number is unity for all various directions of the TSNFL cavity walls if it compared with the corresponding isotherm contours when the Richardson number is very low. This is because the intensity of circulation reduces due to decrease the effect of the vortices coming from the shear force effect when the Richardson number is unity. The thermal energy inside the cavity is transferred by conduction. This can be observed from approximately horizontal and parallel lines instead of convection at the case when the Richardson number is very low.

4.3. The natural convection effect , (i.e., Ri = 100)

Figures **7** and **8** show the streamlines and isotherms when the forced convection effect is less than the natural convection effect (i.e., Ri =100) for various TSNFL cavity orientations. In this case, the shear force has a slight influence compared with the buoyancy force. The results are discussed as follows :-

1-It is clearly seen that when the upper wall moves to the left and when the right side wall moves downwards , the flow field is characterized by a large major vortices which occupy most size of the cavity. The vortices are rotate inside the cavity with the direction of the TSNFL cavity walls. The another major vortices which are observed when the Richardson number is very low (i.e., Ri = 0.01) begin to vanish rapidly and clearly. The reason of this behavior is due to the slight

effect of the shear force when the Richardson number is high. This leads to decrease the vortices which are constructed due to the shear force effect. Therefore , the other major vortices which are constructed due to the buoyancy force take an important role and begin to grow significantly. From the other hand, it can be observed a small minor vortices adjacent to the right side wall. A similar phenomena can be seen when the direction of the movements of the TSNFL cavity walls diverges (for example, when the upper wall moves to the right and the left side wall moves downwards or when the lower wall moves to the right and the left side wall moves upwards , etc.). The maximum stream function at these cases is about ($\Psi_{Max} = 0.00789$).

2- When the direction of the movements of the TSNFL cavity walls converges (for example, when the upper wall moves to the right and the right side wall moves upwards or when the upper wall moves to the left and the left side wall moves upwards , etc.) , the flow inside the cavity can be represented by a large major vortices which cover the majority of the cavity. In this case , the minor vortices are begin to enlarge in size compared with the corresponding minor vortices when the direction of the movements of the TSNFL cavity walls diverges. The maximum stream function at these cases is about ($\Psi_{Max} = 0.00791$).

3- When the direction of the movements of the TSNFL cavity walls is in the clockwise direction (for example, when the lower wall moves to the left and the right side wall moves downwards or when the upper wall moves to the right and the right side wall moves downwards , etc.) , the flow field can be represented also by a single major vortices which move in the clockwise direction. The major difference in this case is that the vortices center begins to shift in upwards or downwards orientations depending on the direction of the movements of the TSNFL cavity walls. Moreover, the minor vortices begin to disappear from the flow field. The maximum stream function at these cases is about ($\Psi_{Max} = 0.00870$). A similar behavior can be noticed when the direction of the movements of the TSNFL cavity walls is in the anti-clockwise direction. The maximum stream function at these cases is about ($\Psi_{Max} = 0.00871$). With respect to isotherms, it is noticeable that they are equally distributed in the cavity as a horizontal lines and the conduction heat transfer is dominant. This is because , when the Richardson number is high (i.e., Reynolds number is low) the temperature gradient decreases and a thermal boundary layers begin to construct and as a result the rate of heat transfer decreases. Furthermore, when the Reynolds number is low, the shear force effect due to the movements of the TSNFL cavity walls decreases and the transferred thermal energy by it decreases which leads to decrease the rate of heat transfer and making the isotherms similar to that are countered in the conduction heat transfer.

4.4. Average Nusselt number effects

Figure **9** shows the average Nusselt number distribution along the hot lower wall for various TSNFL cavity orientations as a function of Richardson number. It can be observed that , the average Nusselt number has a large value when the Richardson number is low (i.e., in the forced convection-dominant region). This behavior can be observed for different TSNFL cavity orientations. The reason of this behavior is due to high intensity of circulation comes from major and minor vortices when the Richardson number is low. Furthermore , the average Nusselt number distribution along the hot bottom wall has a larger value for the following situations :-
For **case I** , when the direction of the movements of the TSNFL cavity walls is in the clockwise direction (i.e., when the upper wall moves to the right and the right side wall moves downwards)
For **case II** , when the movements of the TSNFL cavity walls is in the anti-clockwise direction (i.e., when the upper wall moves to the left and the left side wall moves downwards).
For **case III** , when the movements of the TSNFL cavity walls is in the anti-clockwise direction (i.e., when the lower wall moves to the right and the right side wall moves upwards).
For **case IV** , when the direction of the movements of the TSNFL cavity walls is in the clockwise direction (i.e., when the lower wall moves to the left and the left side wall moves upwards).

The reason of this phenomena is due to strong flow motion at these situations which causes to increase the average Nusselt number values. Therefore, it can be concluded from these results that the rate of heat transfer increases when the movements of the TSNFL cavity walls are in the clockwise or anti-clockwise directions. It is also observed from Figure **9** , that the average Nusselt number distribution along the hot lower wall decreases when the Richardson number increases (i.e., in the natural convection-dominant region).No significant effect of the movements of the TSNFL cavity walls can be observed on the average Nusselt number values when the Richardson number is high (i.e., in the natural convection-dominant region).

5. Conclusions.

1-When the forced convection is significant (Ri << 1), and the direction of the movements of the TSNFL cavity walls converges, the intensity of flow field circulation is enhanced. It is seen that a higher stream function can be obtained in comparison with the among other cases. Generally, the flow field is represented by a two large major and minor vortices.

2-When the forced convection effect is significant , the isotherm contours explain that the flow field in the cavity core is not influenced strongly by the temperature gradient. The isotherm contours take a confusion shape and the convection is dominant. Also, a thermal boundary layer is observed adjacent the hot lower wall.

3-When the forced convection effect is approximately equivalent to the natural convection effect (i.e., Ri =1), the flow field is characterized by two major vortices which are symmetrical in shape but they are different in size. This behavior is seen when the direction of the movements of the TSNFL cavity walls diverge and converge respectively. From the other hand, when the direction of the movements of the TSNFL cavity walls rotate in clockwise and anti-clockwise directions, the flow field is represented by a large single major vortices. In general, the minor vortices are decrease in size and vanish gradually.

4-The disturbance in the isotherms begins to decrease gradually when the Richardson number is unity for all various directions of the TSNFL cavity walls and the conduction heat transfer regime has become the dominant mode of energy transport in the cavity.

5-When the natural convection effect is significant (Ri >> 1), the flow field can be represented by a large single major vortices which occupy most of the cavity. Also a small minor vortices can be noticed at various locations in the cavity.

6- The intensity of circulation and the maximum stream function decreases when the Richardson number increases. Also, the thermal energy transport decreases and the isotherms shape are similar to that found in the conduction heat transfer phenomena.

7-The results indicated various shapes of major and minor vortices for different directions of the movements of the TSNFL cavity walls.

8- The average Nusselt number increases along the hot bottom wall for low values of the Richardson number. As the Richardson number increases, the average Nusselt number decreases.

9- The heat transfer rate increases when the movements of the TSNFL cavity walls are in the clockwise or anti-clockwise directions.

References

1- Moallemi, M. and Jang, K. Prandtl number effects on laminar mixed convection heat transfer in a lid-driven cavity, International Journal of Heat and Mass Transfer ,Vol. 35,1992, pp: 1881–1892.

2- Alleborn, N., Raszillier, H. and Durst, F. Lid-driven cavity with heat and mass transport, International Journal of Heat and Mass Transfer ,Vol. 42,1999, pp: 833–853.

3- Mahapatra,S., Nanda, P. and Sarkar,A. Interaction of mixed convection in two-sided lid driven differentially heated square enclosure with radiation in presence of participating medium, Heat and Mass Transfer,Vol. 42, 2006 , pp : 739–757.

4- Wahba, E. Bifurcation phenomena for two-sided non-facing lid driven cavity flow, WSEAS International Conference on Engineering Mechanics Structures, Engineering Geology (EMESEG '08), Heraklion , Crete Island, Greece, July 22-24, 2008, pp : 111-116.

5- Wahba, E. Multiplicity of states for two-sided and four-sided lid driven cavity flows, Computers and Fluids ,Vol. 38, 2009, pp: 247–253.

6- Alinia, M., Ganji, D. and Gorji-Bandpy, M. Numerical study of mixed convection in an inclined two sided lid-driven cavity filled with nanofluid using two-phase mixture model, Under Press in International Communications in Heat and Mass Transfer , 2011.

7- Mansour, R. and Viskanta, R. Shear opposed mixed convection flow and heat transfer in narrow, vertical cavity, International Journal of Heat and Fluid Flow , Vol. 15, No.6, 1994, pp: 462–469.

8-Oztop, H. and Dagtekin, I. Mixed convection in two sided lid-driven differentially heated square cavity, International Journal of Heat and Mass Transfer ,Vol. 47, 2004, pp:1761–1769.

9- Mahapatra, S., Sarkar, A. and Sarkar, A. Numerical simulation of opposing mixed convection in differentially heated square enclosure with partition , International Journal of Thermal Sciences ,Vol. 46, 2007, pp: 970–979.

10- Luo, W. and Yang, R. Multiple fluid flow and heat transfer solutions in a two-sided lid-driven cavity , International Journal of Heat and Mass Transfer ,Vol. 50, 2007, pp: 2394–2405.

11-Beya,B. and Lili, T. Three-dimensional incompressible flow in a two-sided non-facing lid-driven cubical cavity, Comptes Rendus Mecanique ,Vol. 336, 2008, pp : 863–872.

12- Siegmann-Hegerfeld, T., Albensoeder, S. and Kuhlmann , H. Two and three-dimensional flows in nearly rectangular cavities driven by collinear motion of two facing walls , Experimental Fluids ,Vol. 45, 2008, pp : 781–796.

13-Basak, T., Roy, S., Sharma , P. and Pop, I. Analysis of mixed convection flows within a square cavity with linearly heated side wall(s), International Journal of Heat and Mass Transfer ,Vol. 52, 2009, pp : 2224–2242.

14- Noor,D. , Kanna, P.and Chern, M. Flow and heat transfer in a driven square cavity with double-sided oscillating lids in anti-phase, International Journal of Heat and Mass Transfer ,Vol. 52, 2009, pp : 3009–3023.

15- Ouertatani,N. , Cheikh, M. , Beya , B. , Lili , T. and Campo, A. Mixed convection in a double lid-driven cubic cavity, International Journal of Thermal Sciences ,Vol. 48, 2009, pp : 1265–1272.

16-Cheng and Liu, W. Effect of temperature gradient orientation on the characteristics of mixed convection flow in a lid-driven square cavity , Computers and Fluids ,Vol.39,2010, pp: 965–978.

17-Oueslati , F., Beya,B. and Lili, T. Aspect ratio effects on three-dimensional incompressible flow in a two-sided non-facing lid-driven parallelepiped cavity, Comptes Rendus Mecanique ,Vol. 339, 2011, pp : 655–665.

18- Vicente,J. , Rodriguez, D., Theofilis, V. and Valero, E. Stability analysis in span wise-periodic double-sided lid-driven cavity flows with complex cross-sectional profiles, Computers and Fluids ,Vol. 43, 2011, pp :143–153.

19- Golkarfard,V. , Nasab, S., Ansari, A. and Bagheri, G. Numerical investigation on deposition of solid particles in a lid-driven square cavity with inner heated obstacles, Under Press in Advanced Powder Technology , 2011.

20- Cheng,T. Characteristics of mixed convection heat transfer in a lid-driven square cavity with various Richardson and Prandtl numbers , International Journal of Thermal Sciences, Vol.50, 2011, 197-205.

21- Liu, G. and Quek, S. The Finite Element Method: A Practical Course , Butterworth-Heinemann Publisher , 2003.

Nomenclature:

Symbol	Description	Unit
g	Gravitational acceleration	m/s^2
Gr	Grashof number	
$\overline{Nu}$	Average Nusselt number	
P	Dimensionless pressure	
p	Pressure	N/m^2
Pr	Prandtl number (ν/α)	
Re	Reynolds number	
Ri	Richardson number	
T	Temperature	°C
U	Dimensionless velocity component in x-direction	
V_c	Constant moving velocity	m/s
u	Dimensional velocity component in x-direction	m/s
V	Dimensionless velocity component in y-direction	
v	Dimensional velocity component in y-direction	m/s
X	Dimensionless Coordinate in horizontal direction (x / H)	
x	Cartesian coordinate in horizontal direction	m
Y	Dimensionless Coordinate in vertical direction (y / H)	
y	Cartesian coordinate in vertical direction	m
Greek symbols		
α	Thermal diffusivity	m^2/s
β	Volumetric coefficient of thermal expansion	K^{-1}
θ	Dimensionless temperature	
ν	Kinematic viscosity of the fluid	m^2/s
ρ	Density of the fluid	kg/m^3
Ψ	Dimensionless stream function	
∇	Laplacian operator	
subscripts		
c	Cold	
h	Hot	
x	First derivative in X-direction	
y	First derivative in Y-direction	
Abbreviations		
FEM	Finite element method	
Max	Maximum	
TSNFL	Two sided non-facing lid-driven	
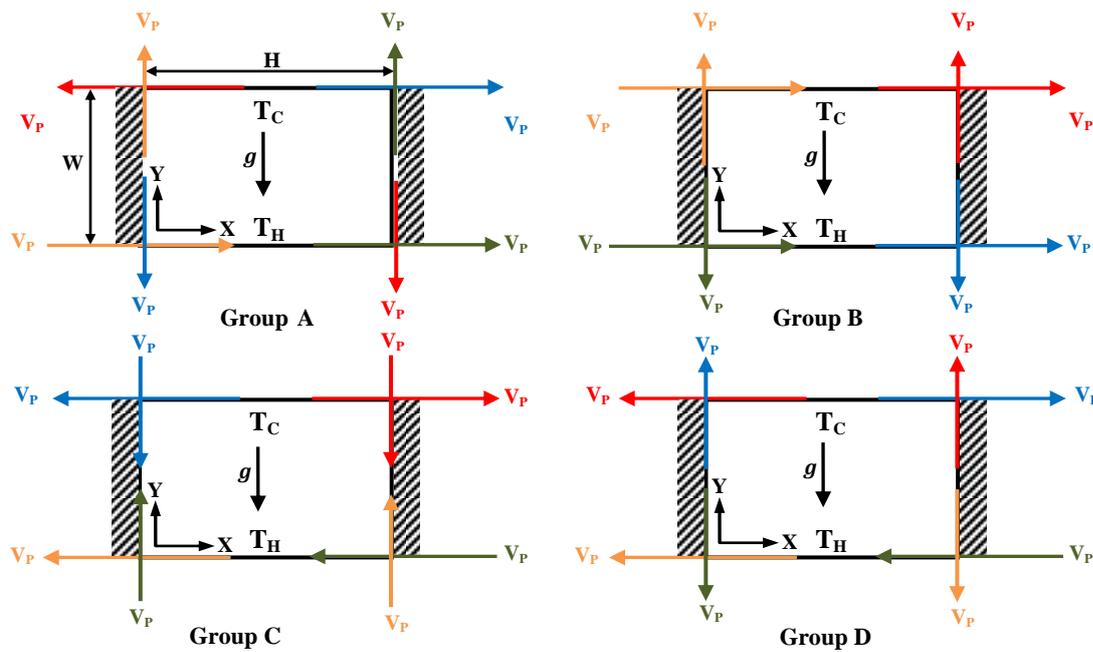
Each group contains four cases of case I ➡, case II ➡, case III ➡ and case IV ➡

Fig. 1. Schematic diagram of the TSNFL cavity for the four cases per each group with boundary conditions.
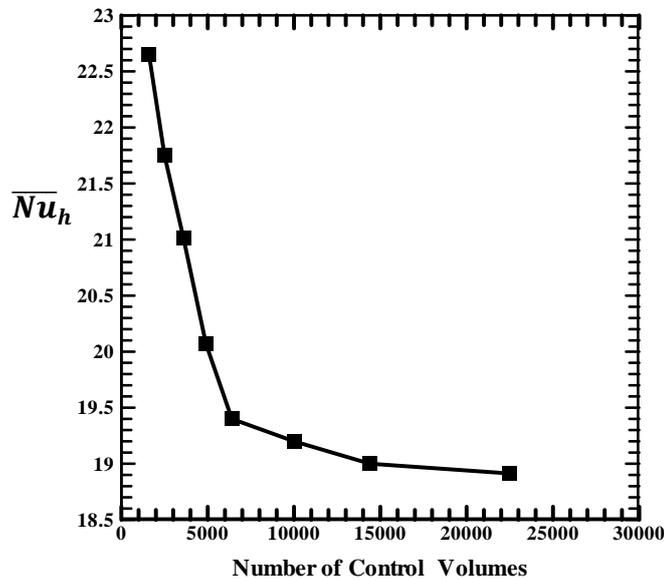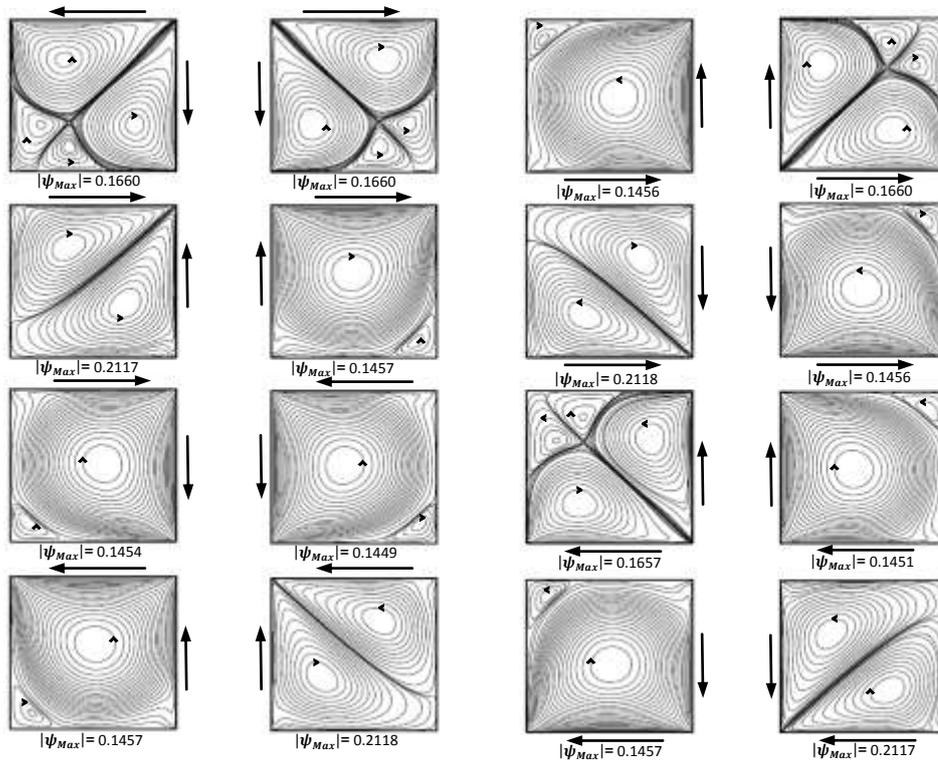

Fig.2 Convergence of average Nusselt number
along the hot lower wall with grid refinement
at Re=1000, Pr = 0.71,Ri= 0.01, case :III.

Table 1
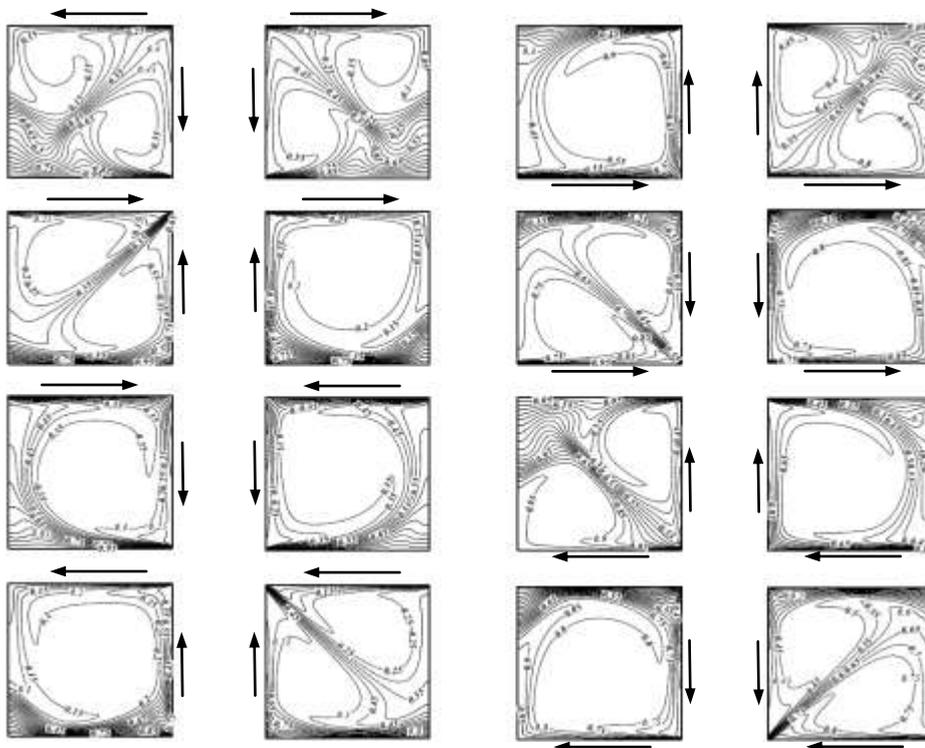
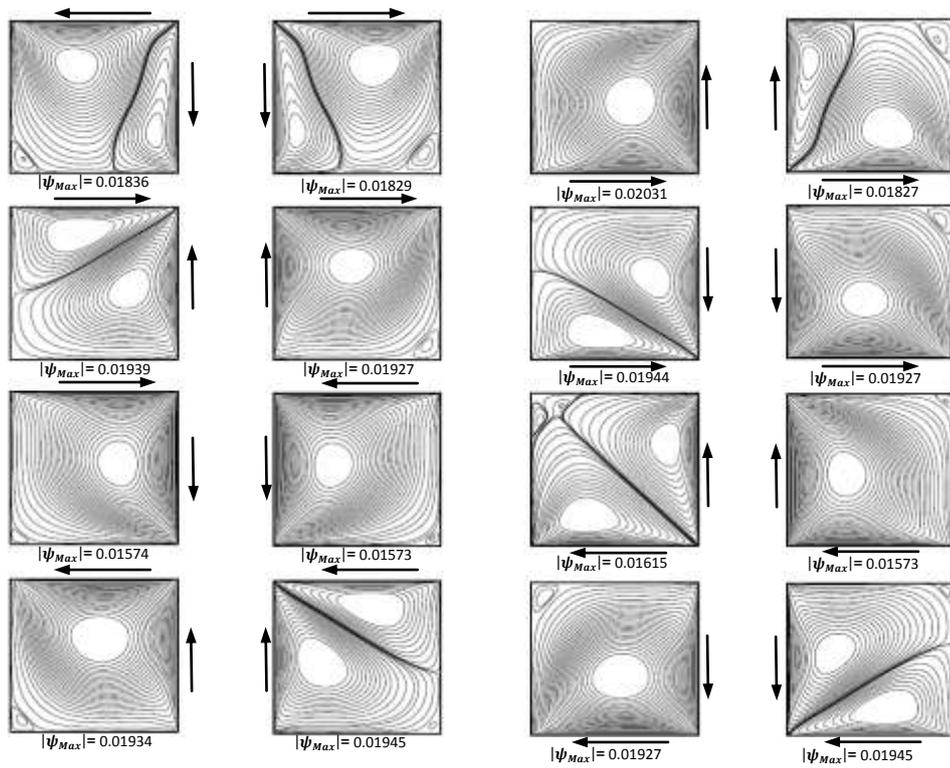Comparison of average Nusselt number values at the top wall with those of previous studies.

Ri	**Oztop** and **Dagtekin [8]**	**Present study**	Max. Error %
1.00	1.33	1.33	-0.746
0.0625	3.60	3.61	0.277
0.01	6.21	6.23	-0.953

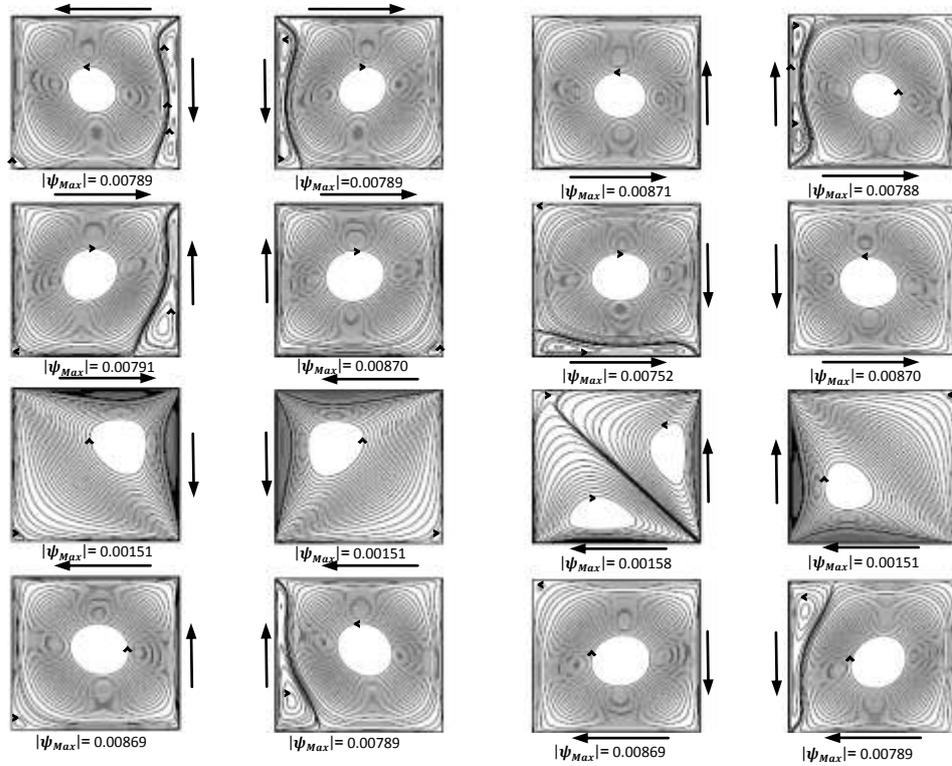**Fig. 3.** Variations of streamlines for different TSNFL cavity orientations at Ri= 0.01

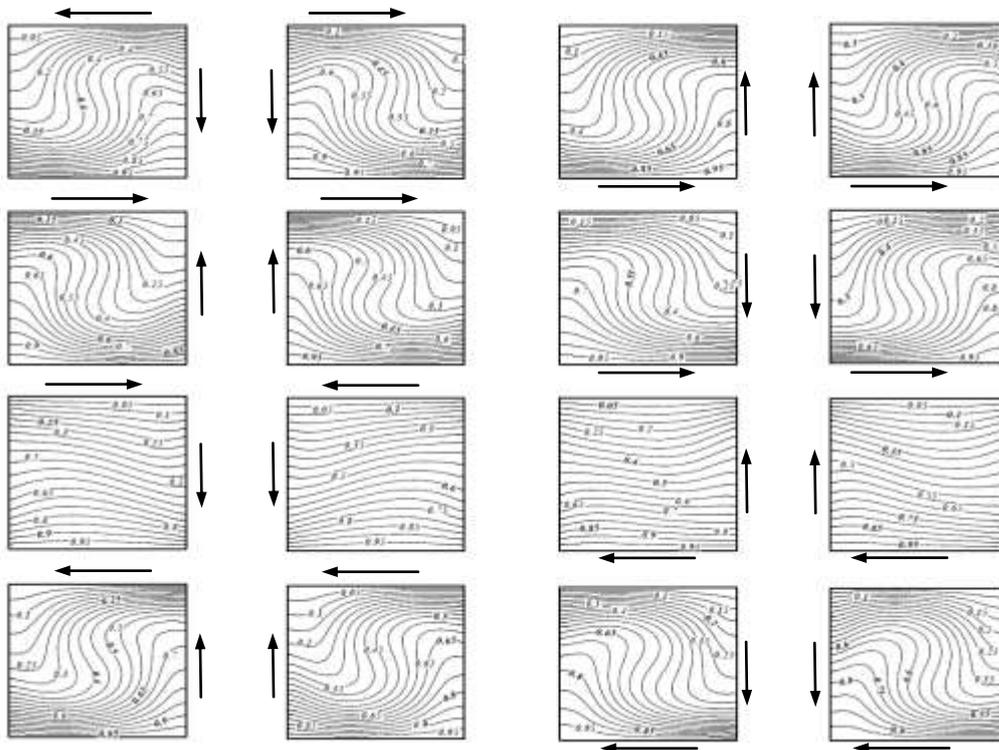**Fig. 4.** Variations of isotherms for different TSNFL cavity orientations at Ri= 0.01

Fig. 5. Variations of streamlines for different non-facing lid driven cavity orientation**s** at Ri= 1
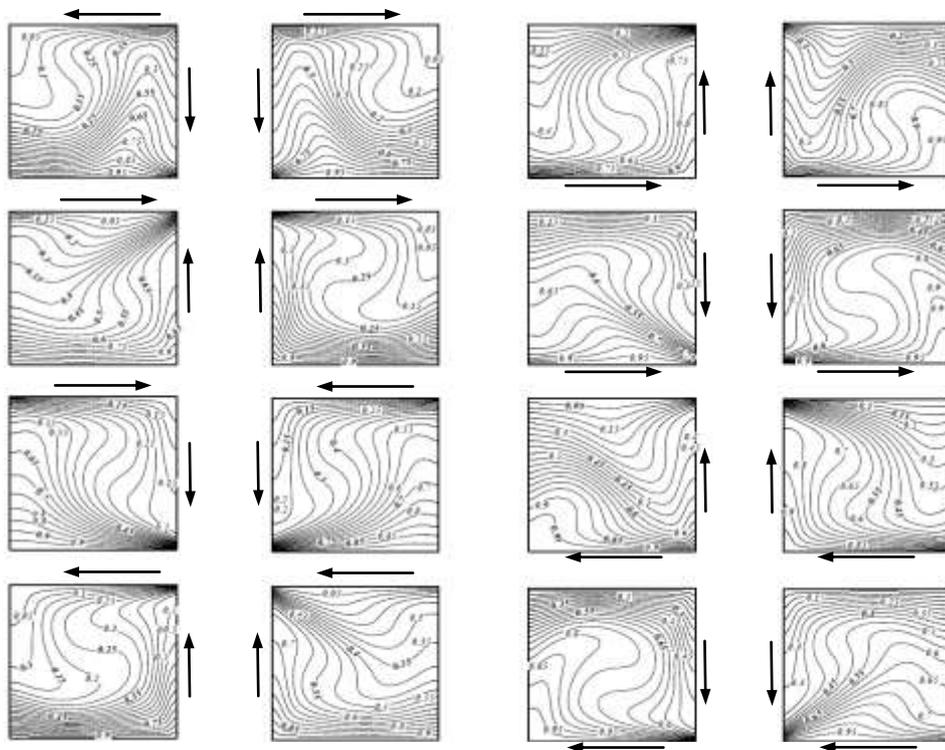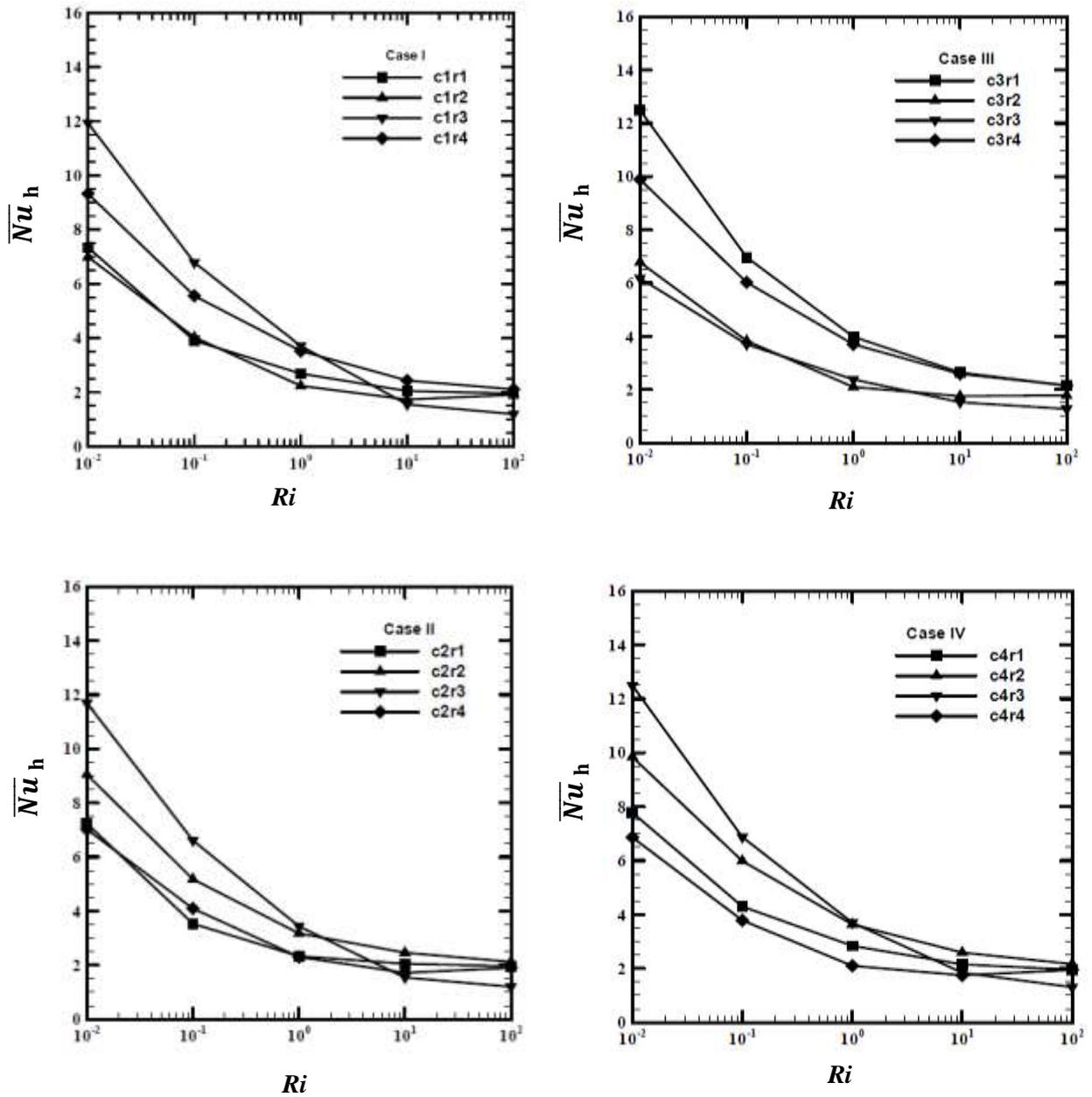
Fig. 6. Variations of isotherms for different non-facing lid driven cavity orientation**s** at Ri= 1

Fig. 7. Variations of streamlines for different non-facing lid driven cavity orientation**s** at Ri= 100

Fig. 8. Variations of isotherms for different non-facing lid driven cavity orientation**s** at Ri= 100

Fig. 9. Average Nusselt number for different cases as a function of Richardson number.